

# THE COMMISSIONING OF THE HALL-B BEAMLINE OF JEFFERSON LAB FOR COHERENTLY PRODUCING A BEAM OF LINEARLY-POLARIZED PHOTONS

P.L. COLE,\* J. KELLIE, F.J. KLEIN, K. LIVINGSTON, J.A. MUELLER,  
J.C. SANABRIA, AND D.J. TEDESCHI, COSPOKESPERSONS OF G8

*\*University of Texas at El Paso, El Paso, TX 79968;*

*Jefferson Lab, Newport News, VA 23606*

*E-mail: cole@jlab.org*

FOR THE CLAS COLLABORATION

The set of experiments forming the g8 run took place this past summer (6/04/01 – 8/13/01) in Hall B of Jefferson Lab. These experiments made use of a beam of linearly-polarized photons produced through coherent bremsstrahlung and represent the first time such a probe has been employed at Jefferson Lab. Among the several new and upgraded Hall-B beamline devices commissioned prior to the production running of g8a were the photon tagger, the coherent bremsstrahlung facility (goniometer + an instrumented collimator), a photon profiler, and the PrimEx dipole + pair spectrometer telescopes. We essentially commissioned a new beamline for photon running in Hall B. The scientific purpose of g8 is to improve the understanding of the underlying symmetry of the quark degrees of freedom in the nucleon, the nature of the parity exchange between the incident photon and the target nucleon, and the mechanism of associated strangeness production in electromagnetic reactions. With the high-quality beam of the tagged and collimated linearly-polarized photons and the nearly complete angular coverage of the Hall-B spectrometer, we seek to extract the differential cross sections and polarization observables for the photoproduction of vector mesons and kaons at photon energies ranging between 1.1 and 2.25 GeV. For the first phase of g8, i.e. g8a, we collected approximately 1.8 billion triggers for  $1.75 \leq E_\gamma \leq 2.25$  GeV. In this paper, we report on the results of the commissioning of the beamline devices for the g8a run.

## 1 Motivation

From our set of experiments on vector-meson photoproduction for the g8 run,<sup>1,2,3</sup> we seek to study the evolution of the spin density matrix elements as functions of the Mandelstam variables,  $s$  and  $t$ , in the effort to extract spin-parity information on the underlying baryon resonances which decay through the  $\rho$  or  $\omega$  channel and the nature of the parity exchange for  $\phi$  production near threshold. With linearly-polarized photons, one has access to nine independent spin density matrix elements. Combinations of which correspond to

the vector-meson polarization,<sup>a</sup> the beam asymmetry  $\Sigma$ , the parity asymmetry  $P$ , and beam-vector meson double polarization observables. In the case of  $s$ -channel helicity conservation or natural parity exchange ( $J^\pi = 0^+, 2^+$ ), the decay angular distribution is given by  $P_\gamma \sin^2 \theta \cos 2\Psi$ ,<sup>b</sup> which corresponds to  $\Sigma = P = 1$ . Whereas for unnatural-parity exchange ( $J^\pi = 0^-$ ), the parity asymmetry flips to  $-1$ . Linearly-polarized photons therefore serve as a parity filter. It is by extracting these density matrix elements as functions of the Mandelstam variables,  $s$  and  $t$ , that we shall obtain a *model-independent* pool of data. These density matrix elements form the meeting ground between theory and experiment. Through their models, theorists predict the helicity amplitudes, and from the decay angular distribution data, experimentalists extract the *bilinear combinations of these helicity amplitudes* or the *density matrix elements*. Accurate and precise measurements of the evolution of these density matrix elements over a wide range of  $s$  and  $t$  will constrain the theory, and thereby give insight into the underlying production mechanisms. For recent information on vector meson production, we refer the reader to the papers<sup>4,5</sup> in these conference proceedings

In the case of the hyperon production, employing the probe of linearly-polarized photons, together with measuring the polarization of the recoil hyperon, gives access to the beam asymmetry  $\Sigma$  and the beam-recoil double polarization observables  $O_{x'}$ ,  $O_{y'}$  and  $O_{z'}$ . These data from the g8 run,<sup>6</sup> coupled with the CLAS-g1<sup>7</sup> data from unpolarized and circularly-polarized photon beams, will provide an almost complete description of the  $\gamma p \rightarrow K^+ \Lambda$  channel and will facilitate a *model-independent* analysis towards identifying the intermediate resonances.

At present there exist conflicting interpretations of the  $\gamma p \rightarrow K^+ \Lambda$  cross section data from SAPHIR.<sup>8</sup> A calculation from Mart and Bennhold<sup>9</sup> interprets the structure at  $W = 1900$  to be the result of one of the ‘missing’ resonances,  $[D_{13}]_3(1960)$ . Saghai and collaborators,<sup>10,11,12</sup> have taken another tack; in their approach they include off-shell effects and  $\Lambda^*$ -exchange and take only the known  $N^*$  resonances into account. The measurement of polarization observables is necessary for settling this issue of the presence or absence of the  $[D_{13}]_3(1960)$ .

---

<sup>a</sup>By means of the decay of the spin-1 vector mesons into the spin-0 pseudoscalars, one gains access to the the tensor polarization components  $T_0^2$ ,  $T_{\pm 1}^2$ , and  $T_{\pm 2}^2$ . Additional information on the polarization observables can be found in Refs.<sup>13,14</sup>

<sup>b</sup>Here,  $\Psi$  is the angle between the direction of the photon polarization vector and the azimuth of the decay plane.

## 2 Brief Theoretical Background on Coherent Bremsstrahlung

The technique of obtaining linearly-polarized photons has been successfully employed at SLAC<sup>16</sup> and Mainz.<sup>17</sup> Detailed discussions of the underlying theory of coherent bremsstrahlung can be found in the papers listed in Ref.<sup>18</sup>

For an electron of energy  $E_o$  to radiate a photon of energy  $k$  requires that the momentum  $\vec{q}_e$  be transferred to a nucleus in the crystal lattice. The minimum momentum transfer,  $q_{\min}$ , – for each individual reciprocal lattice vector – scales with increasing photon energy. Only the lattice vectors for which  $q_{\min}$  is less than  $q_e$  may contribute to the coherent process.

$$q_{\min} = \frac{m_e^2 c^3}{2E_o} \frac{x}{1-x} \leq q_e, \quad (1)$$

where  $x$  is the fractional photon energy,  $k/E_o$ . A discontinuity will arise for  $q_e > q_{\min}$ ; thus demarcating the coherent edge for a given lattice vector. In the limit of small goniometer angles, for a diamond crystal we can write<sup>19</sup>

$$\begin{aligned} \theta_v(k-l) - \theta_v(k+l) &= \frac{\sqrt{2}am_e^2c^3}{4\pi\hbar} \frac{1}{E_o} \left( \frac{x}{1-x} \right) \\ &= [57.0 \text{ GeV} - \text{mrad}] \cdot \frac{1}{E_o} \left( \frac{x}{1-x} \right). \end{aligned} \quad (2)$$

Here,  $(h, k, l)$  define the Miller indices of the reciprocal lattice vector and  $a$  is the length of the fundamental cell. In Fig. 1 we plot the theoretical lattice map for the [100] plane of diamond once it is perpendicular to the direction of the electron beam.

The angular distribution of the coherent and incoherent bremsstrahlung photons are very different. Whereas the polar angular distribution of the incoherent bremsstrahlung photons is *independent* of the photon energy

$$\frac{dN(\theta)}{d\theta} = \frac{\theta}{(1+\theta^2)^2}, \quad (3)$$

the emission angle of the coherent bremsstrahlung photons *decreases* with increasing photon energy ( $x \leq x_d$ )

$$\theta^2 = \frac{1-x}{x} \cdot \frac{x_d}{1-x_d} - 1. \quad (4)$$

Here,  $x_d$  is the maximum fractional photon energy for a given setting of crystal. We can make use of the physical fact that the emission angle of the coherent bremsstrahlung photon is correlated with its energy to enhance the

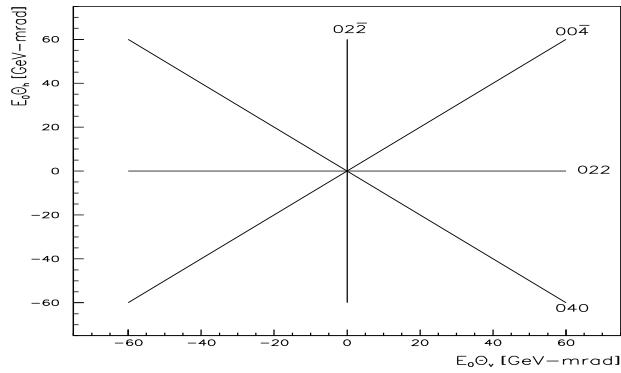


Figure 1. Theoretical lattice map for the [100] plane of diamond, which is approximately perpendicular to the electron beam.

polarization of the beam of photons. We can then extract the spectral peak by tightly collimating the beam and thereby reduce the incoherent background, which further serves to increase the degree of polarization.

### 3 Hall-B Beamline for Producing Linearly-Polarized Photons

The g8 group of experiments employed the coherent bremsstrahlung facility, which was commissioned at the beginning of the g8a run (see Fig. 2). To

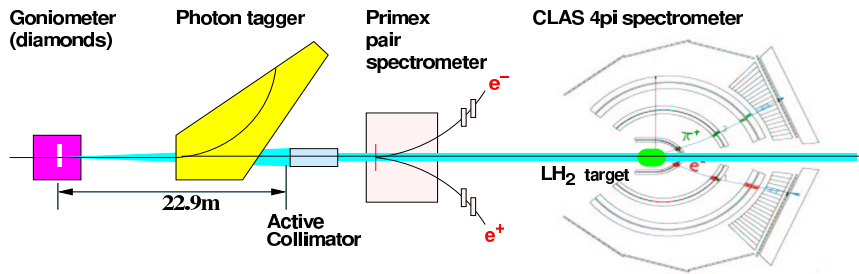


Figure 2. Layout of the Hall-B beamline for the coherent bremsstrahlung facility.

produce polarized photons of energy 2 GeV from an incident 5.7-GeV electron

beam requires that the angle of incidence between the reciprocal lattice vector and the electron beam be aligned to approximately  $1 \mu\text{rad}$ . We employed the GWU goniometer<sup>20</sup> to align the  $50\text{-}\mu\text{m}$  diamond radiator. The technique of Glasgow University for aligning the crystal by means of a series of scans is an extension of Lohman<sup>21</sup> and will be detailed in an upcoming NIM article.<sup>22</sup> The alignment procedure entails executing small angular movements of the crystal and recording the corresponding photon tagger spectrum for each shift in  $\theta_h$  and  $\theta_v$ . The  $[100]$  crystal axis is set at  $60 \text{ mrad}$  from its nominal position and is swept through a  $360^\circ$  cone in azimuth. The procedure for aligning the crystal is shown in Fig. 3, where on the left we show a simulation of a scan that is not yet aligned; the  $\theta_h\text{-}\theta_v$  offset indicates the degree that the  $[100]$  plane is not perpendicular to the electron beam direction. The scan on the right is real data. The dark radial ridges of these plots trace the energy of the coherent peak as the angle between the beam and the face of the crystal varies. As can be seen in the left hand figure, the orientation of the crystal with respect to the beam is found by fitting a template (shown with dashed lines) composed of 8 lines, spaced  $45^\circ$  apart. The final scan is close to a perfect 4-fold symmetry; this shows that the crystal is very well aligned to the beam.

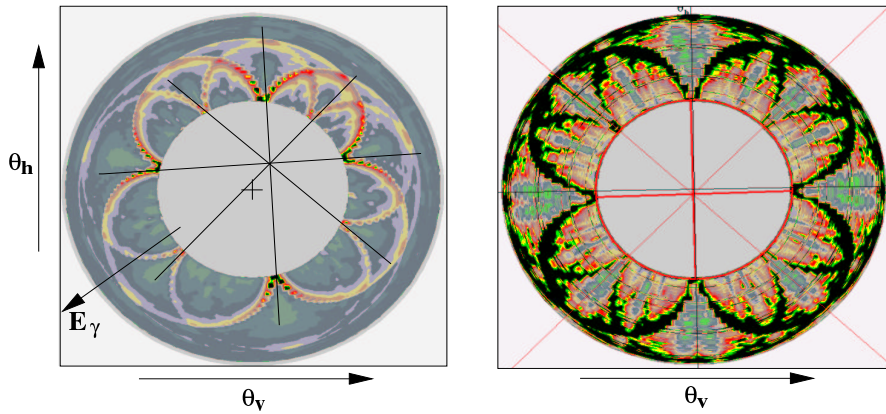


Figure 3. (Left) Simulated scan illustrating the alignment procedure by fitting a template. Here the face of the crystal, i.e. the  $[100]$  plane, is offset in  $\theta_v$  and  $\theta_h$  with respect to the direction of the incident electron beam. (Right) Final scan taken during a data scan run. We see that the crystal is aligned to the desired degree of precision.

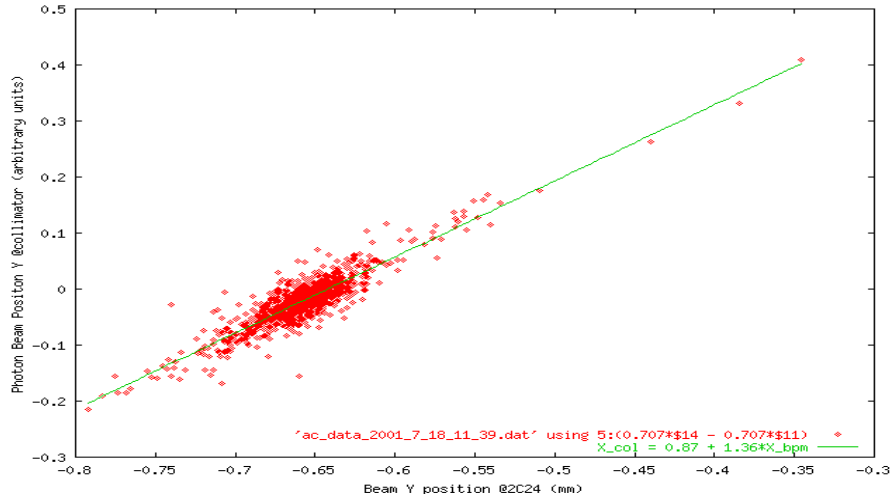


Figure 4. Correlation of the vertical beam position as determined by the embedded collimator scintillators and the beam position monitor. The electron beam position monitor is located 11 m upstream of the collimator, in front of the tagger magnet (2C24). The data were collected on 18 July 2001.

The photon spectrum, as measured by the tagger,<sup>23</sup> is the key diagnostic tool for aligning the reciprocal lattice vectors of the diamond radiator with respect to the incident electron beam to allow for coherent bremsstrahlung production. The focal plane of the photon tagger consists of 384  $\frac{1}{3}$ -overlapping plastic scintillators spanning the energy range of 20 to 95% of the incident electron energy. Each counter thus behaves as an independent detector. From the scan plot on the right in Fig. 3 (see also Fig. 5), we can see that the photon tagger performed very well indeed.

An instrumented collimator<sup>24,25</sup> of aperture 2 mm was installed in the Hall-B beamline downstream of the tagger magnet at a distance of 22.9 m from the diamond radiator. By comparing the asymmetries obtained online from the active elements of the collimator with the electron beam position monitors, we see that the collimator was sensitive to beam shifts to better than 50  $\mu\text{m}$  (see Fig. 4).

## 4 Production Running of g8a

The g8a production running period took place in the summer of 2001 (July 12 – August 13). The energy of the incident electron beam on the 50- $\mu\text{m}$  thick diamond radiator was 5.7 GeV, with a nominal current of 7 nA. For our coherent bremsstrahlung data, we ran at two separate coherent peak edge energies: 2.07 GeV and 2.25 GeV. For understanding and delineating the systematics of the azimuthal dependence of the CLAS detector, we rotated the photon-beam polarization axis by  $90^\circ$  on several occasions. We did this by periodically rotating the diamond crystal between the Miller indices of  $[02\bar{2}]$  and  $[0\bar{2}2]$ , so that these two mutually perpendicular reciprocal lattice vectors were properly aligned with respect to the incident 5.7 GeV electron. To further eliminate misleading or ‘built-in’ azimuthal dependences of the CLAS detector, we took several unpolarized-photon runs employing the amorphous 50- $\mu\text{m}$  thick carbon radiator in lieu of the diamond crystal. These incoherent bremsstrahlung data will furthermore be our yardsticks for determining the polarization of the beam. These complementary data sets will aid us in understanding our azimuthal dependences and thereby will serve to reduce the systematic uncertainties in the differential cross sections of the hyperons and vector mesons.

In Fig. 5 we plot the normalized photon spectrum before and after the collimator. Here, *normalized* means that the spectrum obtained with the diamond radiator is divided by the reference spectrum from an amorphous carbon radiator of thickness 50  $\mu\text{m}$ , and where we have set the baseline to the value of 100. The uncollimated data were collected online with the free-running scalers. The collimated spectrum is derived from TDC hit patterns with the random background subtracted out. This preliminary spectrum results from a first pass through the data with a rough timing calibration. Both data sets, i.e. uncollimated and collimated, are fit with the `anb` code.<sup>26</sup> We see excellent agreement between the data and the fits, and based upon this calculational evidence, we claim we have succeeded in producing a beam of linearly-polarized photons with a high degree of linear polarization of up to a maximum of 84%.

## 5 Summary

With the g8a run, we were able to show ‘proof of principle’ that we can coherently produce a tagged and collimated beam of linearly-polarized photons from a 50- $\mu\text{m}$  diamond radiator. The maximum degree of polarization exceeds 80%. For the first phase of g8, i.e. g8a, we collected approximately

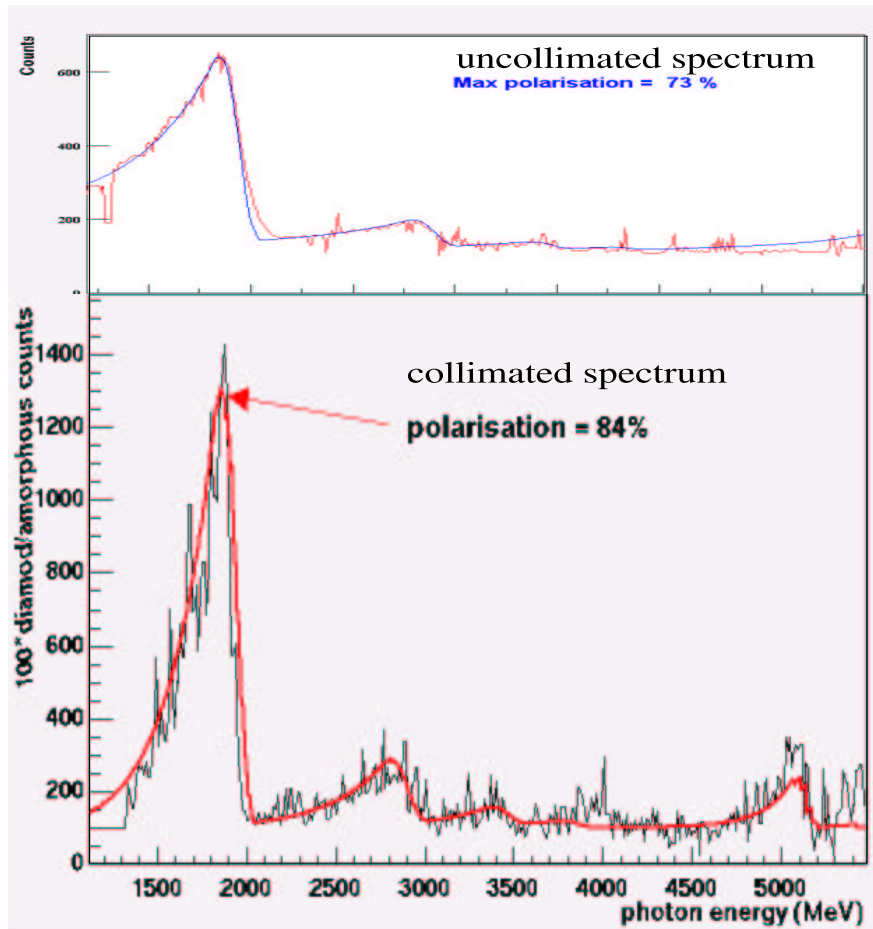


Figure 5. Normalized photon spectra before and after collimation. We remark that both plots have the same vertical scale; this highlights the enhancement of the spectral peak due to the collimation of the photon beam. The fits to both the uncollimated and collimated normalized photon spectra are from the anbc code.<sup>26</sup>

1.8 billion triggers, which, after our data cuts and analysis, should give us well over 100 times the world's data set for  $\rho s$  and  $\omega s$  in the energy range of  $1.75 \leq E_\gamma \leq 2.25$  GeV. We remark that the g8a data set is completely comple-

mentary to those of SPring-8 and GRAAL. SPring-8 strengths lie in the very forward region, GRAAL focuses on neutral-particle detection, and CLAS is designed to measure charged particles in the more central polar-angle regime. The addition of the coherent bremsstrahlung facility to the Hall-B beamline will allow for the cross comparison of the JLab results with those of SPring-8 and GRAAL. In summary, a linearly-polarized photon beam represents a real enhancement of the JLab facility and its physics capabilities.

### Acknowledgments

P.L. Cole wishes to thank Dr. T. Hotta and Prof. T. Nakano of the Research Center for Nuclear Physics of the University of Osaka for their hospitality and is grateful to Prof. M. Fujiwara and the organizers of EMI2001 for inviting him to this thought-provoking conference. This work is supported through grants from the U.S. Department of Energy, the National Science Foundation, and the Engineering and Physical Sciences Research Council of the U.K.

### References

1. "Photoproduction of  $\rho$  Mesons from the Proton with Linearly Polarized Photons," JLab E94-109, P.L. Cole, J.P. Connelly, and K. Livingston, cospokespersons.
2. "Photoproduction of  $\phi$  Mesons with Linearly Polarized Photons," JLab E98-109, D.J. Tedeschi, P.L. Cole, and J.A. Mueller, cospokespersons.
3. "Photoproduction of  $\omega$  Mesons off Protons with Linearly Polarized Photons," JLab E99-013, F.J. Klein and P.L. Cole, cospokespersons.
4. A. Titov and T.-S. H. Lee, "The Role of Low Mass Nucleon Resonances in Near Threshold  $\omega$  Meson Photoproduction," *EMI2001*.
5. Q. Zhao, "Photoproduction of  $\omega$  and  $\phi$  Mesons in the Quark Model," *EMI2001*.
6. "Photoproduction of Associated Strangeness using a Linearly Polarized Beam of Photons," CLAS Approved Analysis 2001-02, J.C. Sanabria, J. Kellie, and F.J. Klein, cospokespersons.
7. "Electromagnetic Production of Hyperons," JLab E89-004, R. Schumacher, spokesperson.
8. SAPHIR Collaboration, M.Q. Tran *et al.*, Phys. Lett. B 445 (1998) 20.
9. T. Mart and C. Bennhold, Phys. Rev. C 61 (2000) 012201.
10. W.-T. Chiang, F. Tabakin, T.-S. H. Lee, and B. Saghai, Phys. Lett. B 517 (2001) 101.

11. Z. Li and B. Saghai, Nucl. Phys. A 644 (1998) 345;  
Z. Li, B. Saghai, T. Ye, and Q. Zhao, *work in progress*.
12. B. Saghai, "Missing Resonance Search via Meson Electromagnetic Production," *EMI2001*.
13. K. Schilling, P. Seyboth, and G. Wolf, Nucl. Phys. B 15 (1970) 397;  
D. Schildknecht and B. Schrempp-Otto, Nuovo Cim. 5A, (1971) 183.
14. C.G. Fasani, F. Tabakin, and B. Saghai, Phys. Rev. C 46 (1992) 2430;  
B. Saghai and F. Tabakin, Phys. Rev. C 53 (1996) 66;  
M. Pichowsky, C. Savkli, and F. Tabakin, Phys. Rev. C 53 (1996) 593;  
C. Savkli, F. Tabakin, and S.N. Yang, Phys. Rev. C 53 (1996) 1132;  
B. Saghai and F. Tabakin, Phys. Rev. C 55 (1997) 917;  
W.M. Kloet, W.-T. Chiang, and F. Tabakin, Phys. Rev. C 58 (1998) 1086.
15. F.J. Klein, Ph.D. thesis, Bonn-IR-96-008 (1996);  
F.J. Klein,  $\pi$ N Newsletters, No. 14 (1998) 141.
16. W. Kaune *et al.*, Phys. Rev. D 11 (1975) 478.
17. D. Lohman *et al.*, Nucl. Instr. Meth. A (1994) 343; J. Peise, M.S. Thesis, Universität Mainz (1989) ; D. Lohman, M.S. Thesis, Universität Mainz (1992); F. Rambo, M.S. Thesis, Universität Göttingen (1995); A. Schmidt, M.S. Thesis, Universität Mainz (1995).
18. F.H. Dyson and H. Überall, Phys. Rev. 99 (1955) 604;  
H. Überall, Phys. Rev. 103 (1956) 1055;  
H. Überall, Phys. Rev. 107 (1957) 223;  
H. Überall, Z. Naturforsch. 17a (1962) 332;  
G. Diambri-Palazzi, Rev. Modern Phys. 40 (1968) 611;  
U. Timm, Fortschr. Phys. 17 (1969) 765;  
R. Rambo *et al.*, Phys. Rev. C 58 (1998) 489.
19. D. Luckey and R.F. Schwitters, Nucl. Instr. and Meth. 81 (1970) 64.
20. NSF Award 9724489, W.J. Briscoe, K.S. Dhuga, and L.C. Maximon, co-PIs, The George Washington University, Washington, D.C., 20052.
21. D. Lohman, M. Schumacher *et al.*, Nucl. Instr. and Meth. A 343 (1994) 494.
22. K. Livingston, to be submitted to Nucl. Instr. and Meth. A.
23. D. Sober *et al.*, Nucl. Instr. and Meth. A 343 (2000) 263.
24. P.L. Cole, "The IPN-Orsay/UTEP Instrumented Collimator," August (1999) 17pp. *unpublished*.
25. A. Puga, M.S. thesis, University of Texas at El Paso, "Calibration of the UTEP/Orsay Instrumented Collimator via the LabVIEW-Benchtop Data Acquisition System," December, 2001.
26. A. Natter, *ANB code*, URL:  
<http://www.pit.physik.uni-tuebingen.de/~natter/software/brems-anb.html>